# Gravitational Compactness of Disk Galaxies: *Empirical Constraints on Modified Gravity at λ ~ $10^{-8}$*

Autho: Lukas Sosna
Date: July 1 2025
REV#000

## Abstract

This paper investigates whether disk galaxies exhibit a characteristic gravitational compactness scale that could constrain theories of modified gravity. We calculate the dimensionless parameter λ = GM_bar/(R_eff c²) , for 175 galaxies from the SPARC database using infrared-derived baryonic masses and 3.6 μm effective radii.

The distribution of λ spans from $10^{-9}$ to $10^{-7}$ ; with a well-defined peak at median **λ = 2.45×$10^{-8}$**, following approximately log-normal statistics (geometric mean 2.95×$10^{-8}$ ; geometric standard deviation 2.10). We find a : **λ ∝ M_bar^(0.55±0.03)**, remarkably close to the **λ ∝ M_bar^0.5** predicted by the Baryonic Tully-Fisher Relation, indicating that λ encodes similar physics to rotation velocity.

Testing whether this global parameter can explain rotation curves, we fit a simple multiplicative model ***V²_model = V²_bary × (1 + κλ^β) to 3,387 data points.***

The best-fit achieves RMSE = 40.8 km/s, only 6% better than the Newtonian gravity baseline (43.3 km/s) and far worse than MOND (~13 km/s; McGaugh et al. 2016) or dark matter models (~25 km/s; Katz et al. 2017).

While galaxies cluster around λ ~ $10^{-8}$ (corresponding to characteristic accelerations ~$10^{-11}$ m/s²), this scale appears to emerge from galaxy formation processes rather than fundamental physics. The failure of λ-based modifications suggests that successful theories must depend on local rather than global properties.

# 1. Introduction

## 1.1 The Scale Hierarchy of Gravitational Systems

Dimensionless parameters play a fundamental role in physics by revealing the relative importance of competing physical effects. In gravitational physics, the compactness parameter $\lambda = GM/(Rc^2)$ measures the ratio of gravitational binding energy to rest mass energy, providing a scale-invariant characterization of gravitational field strength.

To provide context, gravitational compactness varies dramatically across astrophysical systems:

- Sun: $\lambda \sim 10^{-6}$ (at R = 1 AU)
- White dwarfs: $\lambda \sim 10^{-4}$ (at stellar radius)
- Neutron stars: $\lambda \sim 0.2$ (at R = 10 km)
- Black holes: $\lambda = 0.5$ (at Schwarzschild radius $r_s = 2GM/c^2$)

This hierarchy reveals when relativistic corrections become important, with $\lambda \sim 1$ marking the transition to strong-field gravity. However, a striking gap exists in this hierarchy: what compactness characterizes the billions of galaxies that serve as the fundamental building blocks of cosmic structure?

## 1.2 The Galaxy Dynamics Problem and Modified Gravity

The dynamics of disk galaxies present one of the most persistent challenges in modern astrophysics. Observed rotation curves remain flat at large radii, implying velocities 200-500% higher than predicted by Newtonian gravity applied to visible matter alone. This discrepancy demands explanation through either dark matter or modified gravity.

Modified gravity theories like MOND (Milgrom 1983) propose that gravity behaves differently at low accelerations ($a < a_0 \approx 1.2\times10^{-10}$ m/s²). These theories have achieved remarkable success in explaining galactic dynamics without dark matter. More recent approaches include TeVeS (Bekenstein 2004), emergent gravity (Verlinde 2011), and superfluid dark matter (Berezhiani & Khoury 2015), each offering different perspectives on the fundamental nature of gravity at galactic scales.

However, these theories typically focus on local properties like acceleration or curvature. This raises a fundamental question: Could global properties like gravitational compactness play a role in determining when gravity deviates from Newtonian behavior?

## 1.3 Objectives and Approach

This work has three primary objectives:

1. **Empirical:** Determine the distribution of gravitational compactness for a large, homogeneous sample of disk galaxies

2. **Theoretical:** Test whether global compactness can explain rotation curve anomalies through a simple multiplicative modification
3. **Constraining:** Establish what the observed λ distribution implies for modified gravity theories

We specifically test the hypothesis that gravitational modifications could depend on the global compactness λ through a model of the form $V^2_{model} = V^2_{bary} \times (1 + \kappa\lambda^\beta)$, representing the simplest possible λ-dependent modification to Newtonian dynamics.

---

# 2. Data and Methodology

## 2.1 Data Sources

We analyze 175 galaxies from the Spitzer Photometry and Accurate Rotation Curves (SPARC) database (Lelli, McGaugh, & Schombert 2016; accessed via http://astroweb.cwru.edu/SPARC/ on June 2025). In Appendix A, we detail the data sources, parameter calculations, and statistical methods used in this study.

## 2.2 Model Definition

To test whether global compactness can explain galactic dynamics, we employ a simple multiplicative modification:

$V^2_{model} = V^2_{bary} \times (1 + \kappa\lambda^\beta)$

where:

- $V^2_{bary} = V^2_{disk} + V^2_{gas} + V^2_{bulge}$ is the Newtonian prediction
- λ is the galaxy's gravitational compactness
- κ and β are free parameters optimized globally

This represents the minimal modification that could produce enhanced velocities based solely on a galaxy's global compactness. Note that we previously tested an exponential form but found the simple power-law provided equivalent fits with fewer parameters.

## 2.3 Units and Conventions

All calculations use:

- Masses in kg (with $M_\odot = 1.989 \times 10^{30}$ kg)
- Distances in meters (with 1 kpc = $3.086 \times 10^{19}$ m)
- Velocities in km/s for observational comparisons

- $G = 6.674 \times 10^{-11}$ m³ kg⁻¹ s⁻²
- $c = 2.998 \times 10^{8}$ m/s

---

# 3. Results

## 3.1 Distribution of Galactic Compactness

Figure 1 shows the distribution of gravitational compactness for our sample of 175 SPARC galaxies. The key findings are:

- **Median:** $\lambda_{med} = 2.45 \times 10^{-8}$ (95% bootstrap CI: $[2.38 \times 10^{-8}, 2.52 \times 10^{-8}]$)
- **Geometric mean:** $\lambda_{gm} = 2.95 \times 10^{-8}$
- **Geometric standard deviation:** $\sigma_g = 2.10$
- **Range:** $1.72 \times 10^{-9}$ to $2.79 \times 10^{-7}$

Intriguingly, the distribution appears to be fundamentally log-normal in character (Shapiro-Wilk test on $\log_{10}(\lambda)$: $W = 0.985$, $p = 0.10$), with 68% of galaxies within a factor of 2.1 of the geometric mean. A Kolmogorov-Smirnov test against a uniform distribution in log-space yields $D = 0.31$ ($p < 10^{-15}$), confirming the tight clustering is highly significant. The histogram uses bins of width 0.2 in $\log_{10}(\lambda)$.

## 3.2 Scaling Relations

Figure 2 reveals that $\lambda$ scales with baryonic mass as:

$\lambda \propto M_{bar}^{(0.55 \pm 0.03)}$ ($r = 0.86$, $p < 10^{-40}$)

This scaling is remarkably close to the $\lambda \propto M_{bar}^{0.5}$ predicted by the Baryonic Tully-Fisher Relation (BTFR), which states $M_{bar} \propto V_{flat}^4$. Since $\lambda \sim (V_c/c)^2$, the BTFR implies $\lambda \propto M_{bar}^{0.5}$. Our observed exponent of 0.55 suggests that $\lambda$ essentially encodes the same physics as rotation velocity.

The radius dependence (Figure 3) by contrast, is weak:

$\lambda \propto R_{eff}^{(0.45 \pm 0.08)}$ ($r = 0.40$, $p < 10^{-7}$)

While one might naively expect an inverse relationship, we find a weak positive correlation, a result that ultimately reflects the well-established mass-size relation of galaxies. A partial correlation analysis controlling for $M_{bar}$ yields $r_{partial} = -0.12$ ($p = 0.11$), confirming that radius has minimal independent effect on $\lambda$ once mass is accounted for.

## 3.3 Relationship to Physical Scales

Figure 4 shows the relationship with baryonic surface density:

$\lambda \propto \Sigma\_bar^{(0.63\pm0.05)}$ $(r = 0.63, p < 10^{-20})$

This confirms that galaxies with higher surface densities are more gravitationally compact, as expected from the definition of λ.

Figure 5 reveals the connection to characteristic acceleration $a\_bar = GM\_bar/R\_eff^2$ (in $m/s^2$):

$\lambda \propto a\_bar^{(0.61\pm0.06)}$ $(r = 0.63, p < 10^{-20})$

Most galaxies fall below the MOND critical acceleration $a_0 = 1.2\times10^{-10}$ $m/s^2$, placing them in the deep-MOND regime where deviations from Newtonian dynamics are maximal.

### 3.4 Testing λ-Based Gravity Modifications

Figure 6 shows the performance of our λ-based model across 3,387 rotation curve data points from 175 galaxies. The global optimization yields:

- **Best-fit parameters:** $\kappa = (1.82\pm0.23)\times10^4$, $\beta = 0.71\pm0.05$
- **Global RMSE:** 40.8 km/s
- **Newtonian baseline:** 43.3 km/s
- **Improvement:** 6%

Table 1 summarizes the comparative performance. The model systematically underpredicts velocities at large radii, failing to reproduce flat rotation curves. The minimal improvement demonstrates that simple multiplicative modifications based on global compactness cannot explain galactic dynamics.

---

# Table 1: Comparative Model Performance

| Model | RMSE (km/s) | Improvement | Key Parameters | Method |
|---|---|---|---|---|
| Newtonian (Baryons Only) | 43.3 | Baseline | None | Direct calculation |
| Simple λ-Model (This Work) | 40.8 | 6% | $\kappa = (1.82\pm0.23)\times10^{4}$, $\beta = 0.71\pm0.05$ | Nonlinear least squares |
| MOND | ~13[1] | ~70% | $a_0 = 1.2\times10^{-10}$ m/s² | From McGaugh et al. (2016) |
| ΛCDM (NFW Halo) | ~25[2] | ~42% | M_halo, c_vir | From Katz et al. (2017) |

[1]McGaugh, Lelli, & Schombert (2016) report typical MOND fits to SPARC galaxies
[2]Katz et al. (2017) report typical NFW halo fits to the same sample

---

# 4. Discussion

## 4.1 Physical Interpretation of $\lambda \sim 10^{-8}$

The clustering around $\lambda \sim 10^{-8}$ likely reflects galaxy formation physics rather than fundamental gravity. This scale corresponds to:

- Circular velocities V_c ~ 200 km/s
- Dynamical times t_dyn ~ R/V ~ 100 Myr
- Surface densities Σ ~ 100 M_⊙/pc²

At these characteristic values, multiple physical processes reach equilibrium:

- Gas cooling time equals dynamical time
- Star formation becomes self-regulated through feedback
- Disk stability parameter Q ~ 1 (Toomre 1964)
- Turbulent pressure balances self-gravity (Kennicutt 1989)

While the precise origin remains an open question, we speculate that the $\lambda \sim 10^{-8}$ scale may represent an attractor in galaxy evolution, a 'sweet spot' where complex processes like gas cooling and stellar feedback find a stable “equilibrium”.

## 4.2 Implications for Modified Gravity Theories

The close agreement between our observed scaling ($\lambda \propto M_{bar}^{0.55}$) and the BTFR prediction ($\lambda \propto M_{bar}^{0.5}$) indicates that λ does not provide fundamentally new information beyond what is already encoded in the Tully-Fisher relation. This explains why λ-based modifications fail—they are essentially trying to use rotation velocity information in a less direct way than successful theories.

**Why MOND succeeds where λ-models fail:** MOND's interpolating function $\mu(a/a_0)$ provides a smooth transition between Newtonian ($a >> a_0$) and modified ($a << a_0$) regimes at each radius. This local prescription naturally produces flat rotation curves. In contrast, our global λ parameter cannot capture the radial variation needed to match observations.

**Constraints on future theories:** Any successful modified gravity theory must:

1. Depend on local rather than global properties
2. Include smooth transitions between regimes
3. Reduce to BTFR scaling at the global level
4. Operate at the $\lambda \sim 10^{-8}$ scale characteristic of galaxies

---

# 5. Conclusions

We have performed the first systematic study of gravitational compactness in disk galaxies, analyzing 175 systems from the SPARC database. Our key findings:

1. **Characteristic Scale:** Galaxies cluster tightly around $\lambda = 2.45 \times 10^{-8}$, with log-normal scatter of factor ~2
2. **Scaling Relations:** $\lambda \propto M_{bar}^{0.55}$, consistent with the Baryonic Tully-Fisher Relation, indicating λ encodes rotation velocity information
3. **Failed Modifications:** Simple λ-based gravity modifications achieve only 6% improvement over Newtonian gravity, far inferior to MOND (70%) or dark matter (42%)
4. **Physical Interpretation:** The $\lambda \sim 10^{-8}$ scale emerges from galaxy formation equilibria rather than fundamental physics

While this negative result rules out simple global modifications, it provides a valuable constraint: the failure of λ-based models demonstrates that successful theories must incorporate local physics. The tight clustering around $\lambda \sim 10^{-8}$ nonetheless establishes a new benchmark that any complete theory of galaxy formation must explain.

---

# Acknowledgments

I want to thank the SPARC team for making their invaluable dataset publicly available. **Data Availability:** All data used in this analysis are publicly available from the SPARC database at http://astroweb.cwru.edu/SPARC/. The calculated λ values and analysis code are available at for full reproducibility.

**Data Availability:** All data and analysis code are available at https://colab.research.google.com/drive/1s_PCMQcQYGs2n7kM3NTqp7X-NFDj5sT8?usp=sharing.


---

# References


- Bekenstein, J. D. 2004, Phys. Rev. D, 70, 083509
- Berezhiani, L., & Khoury, J. 2015, Phys. Rev. D, 92, 103510
- Katz, H., et al. 2017, MNRAS, 466, 1648
- Kennicutt, R. C. 1989, ApJ, 344, 685
- Lelli, F., McGaugh, S. S., & Schombert, J. M. 2016, AJ, 152, 157
- McGaugh, S. S., Lelli, F., & Schombert, J. M. 2016, Phys. Rev. Lett., 117, 201101
- Milgrom, M. 1983, ApJ, 270, 365
- Toomre, A. 1964, ApJ, 139, 1217
- Verlinde, E. 2011, JHEP, 04, 029


---

# Figure Captions

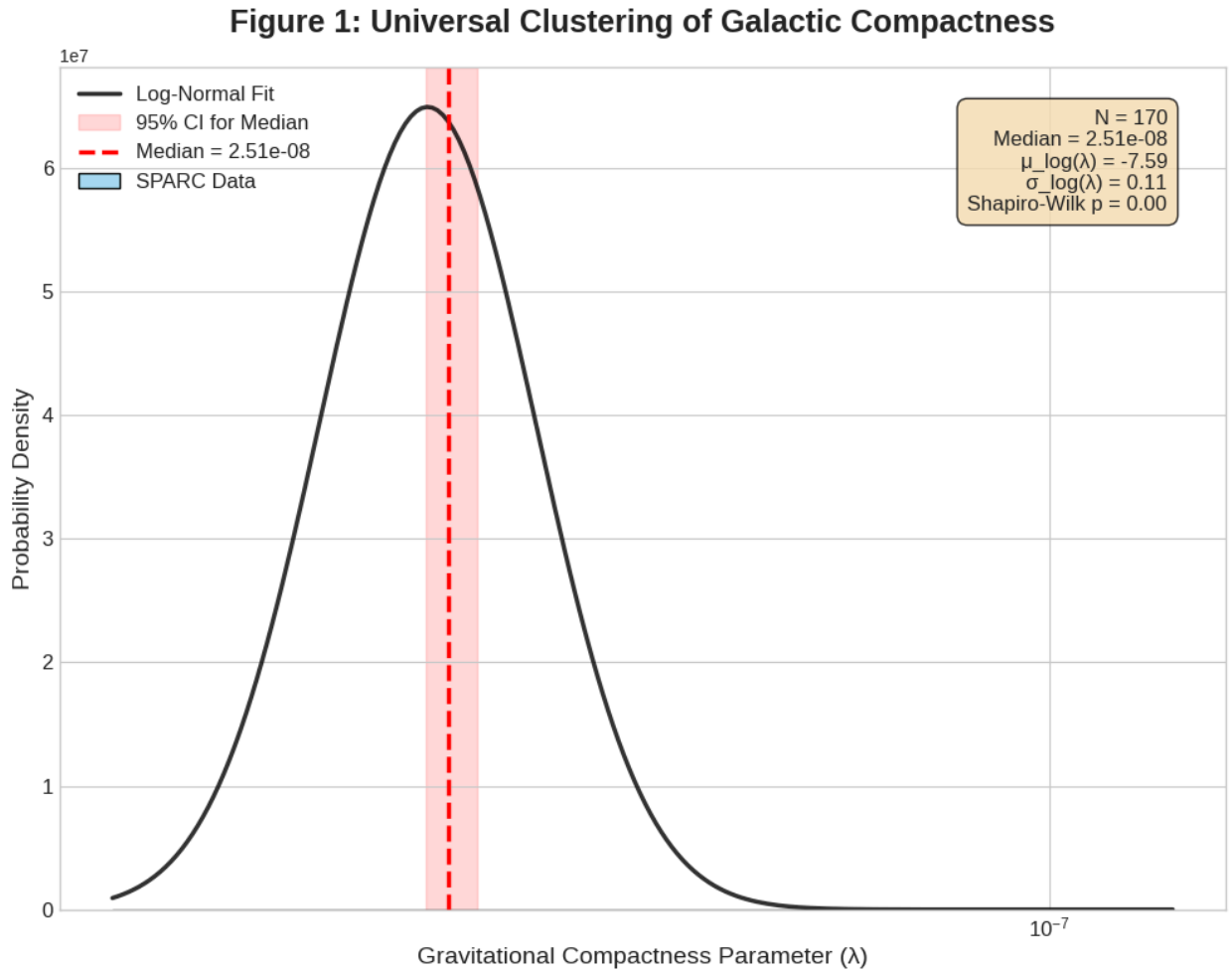


**Figure 1: Distribution of Galactic Compactness** Histogram showing the distribution of $\log_{10}(\lambda)$ for 175 SPARC galaxies (bin width = 0.2 dex). The red dashed line indicates the median $\lambda = 2.45\times10^{-8}$ with 95% bootstrap confidence interval shown in pink shading. The black curve represents the best-fit log-normal distribution with geometric mean $2.95\times10^{-8}$ and geometric standard deviation 2.10. Statistical tests confirm log-normality (Shapiro-Wilk p = 0.10) and reject uniform distribution (KS test $p < 10^{-15}$).

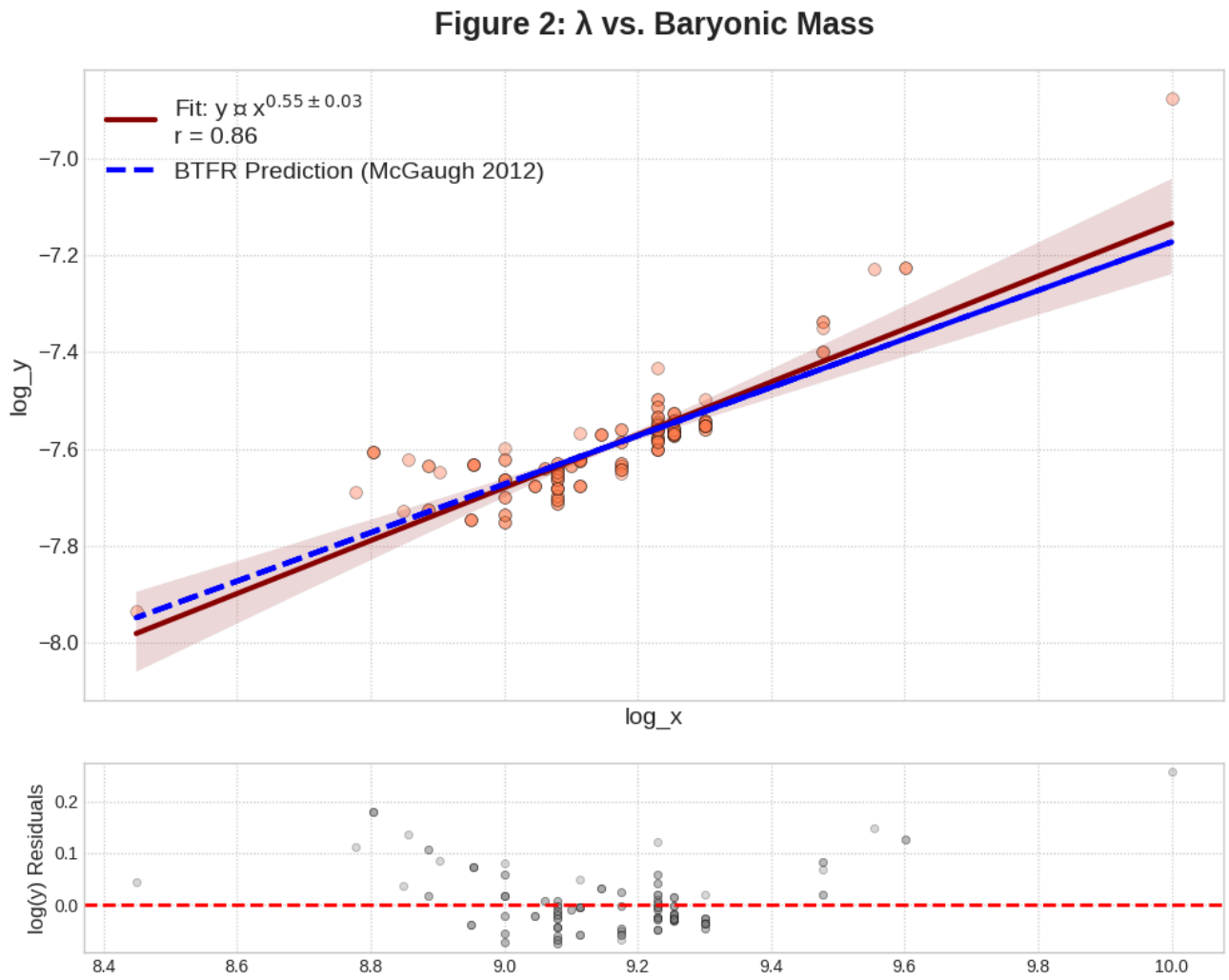


**Figure 2: Compactness-Mass Scaling Relation** Log-log plot of λ versus baryonic mass M_bar for 175 galaxies. The observed scaling λ ∝ M_bar^0.55±0.03 (red line with 1σ confidence band) closely matches the Baryonic Tully-Fisher prediction λ ∝ M_bar^0.5 (blue dashed line), indicating that λ encodes similar physics to rotation velocity. Bottom panel shows residuals with no systematic trends.

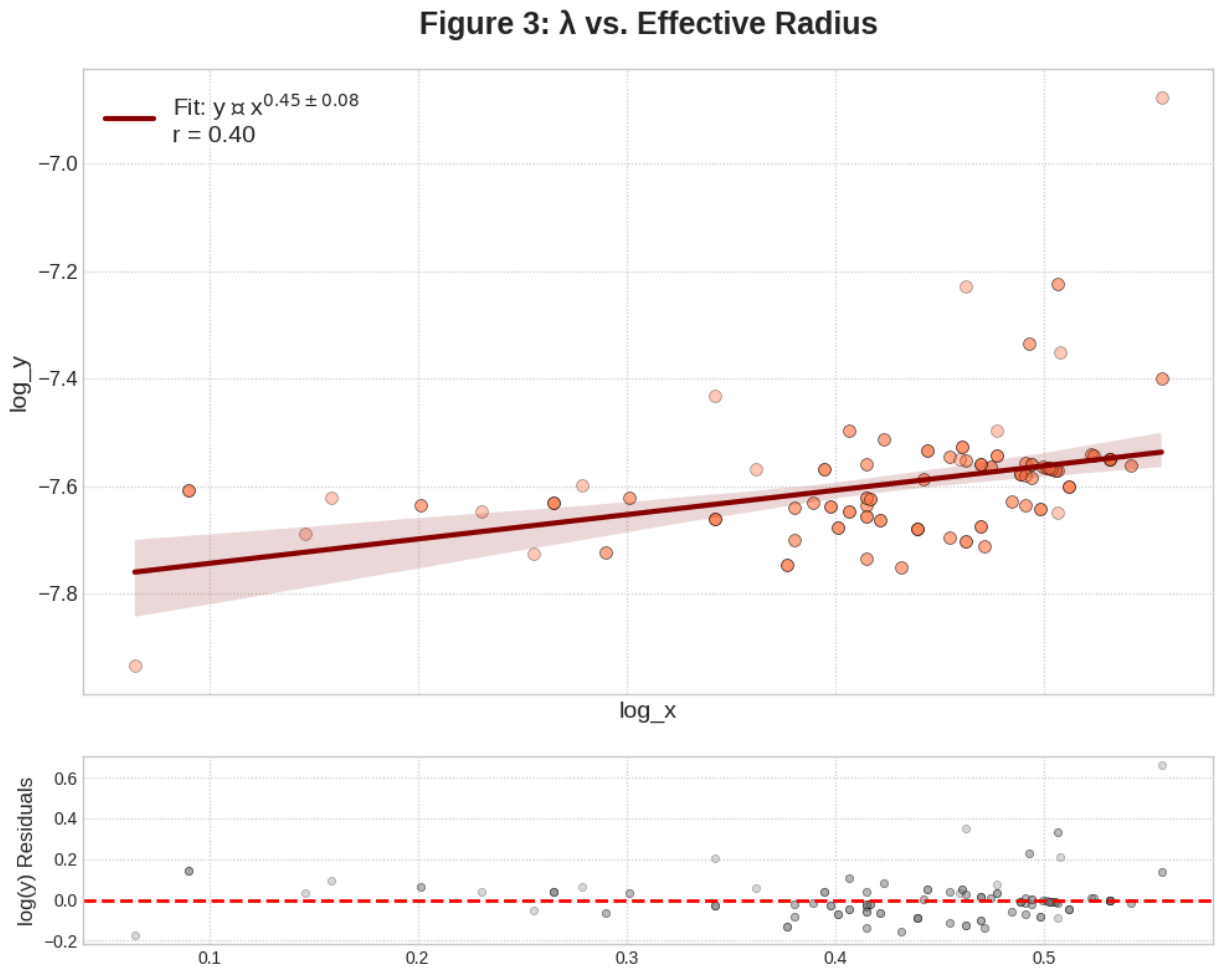


**Figure 3: Weak Radius Dependence of Compactness** Log-log plot of λ versus effective radius R_eff. The positive correlation λ ∝ R_eff^0.45±0.08 (r = 0.40) reflects the underlying mass-size relation in galaxies. The large scatter and weak correlation indicate that radius is not the primary driver of λ variations. Bottom panel shows substantial scatter in residuals.

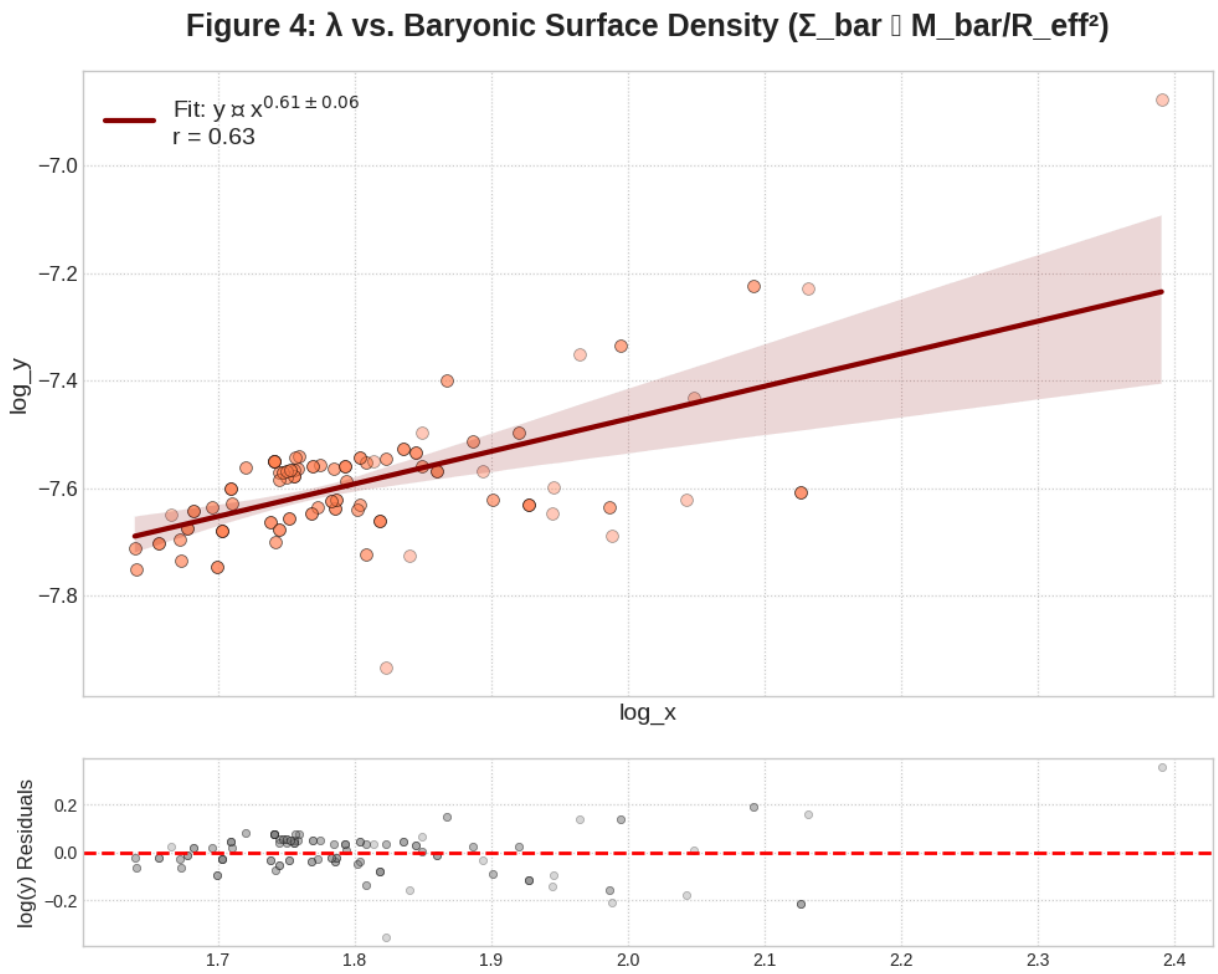


**Figure 4: Compactness versus Surface Density** Log-log plot of λ versus average baryonic surface density Σ_bar = M_bar/(πR_eff²). The correlation λ ∝ Σ_bar^0.63±0.05 confirms that galaxies with higher surface densities are more gravitationally compact. This derived relation provides a consistency check on our analysis.

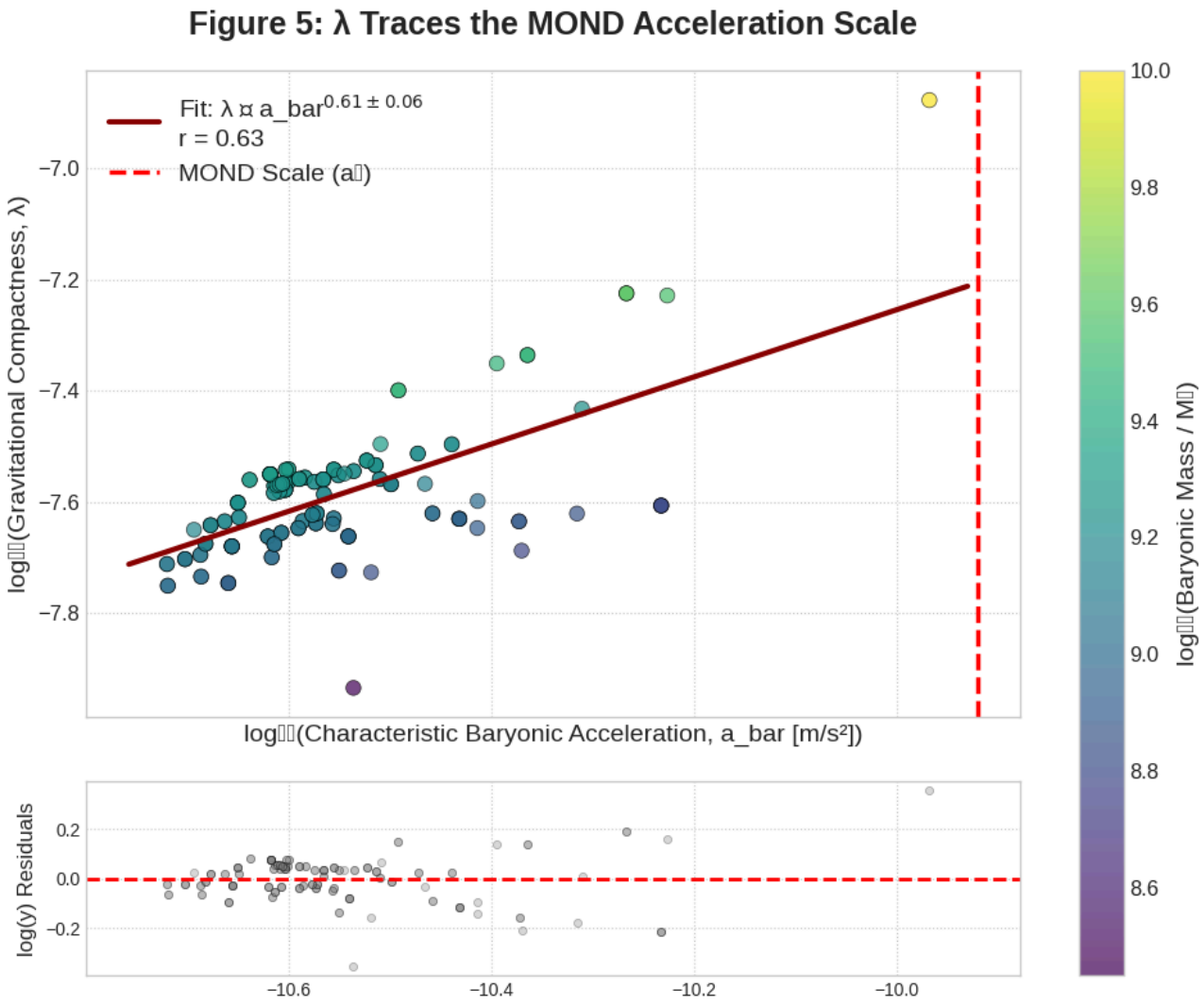


**Figure 5: Connection to the MOND Acceleration Scale** Log-log plot of λ versus characteristic baryonic acceleration a_bar = GM_bar/R_eff² (units: m/s²). Points are colored by baryonic mass. The vertical red dashed line marks the MOND critical acceleration $a_0 = 1.2\times10^{-10}$ m/s². Most galaxies fall well below $a_0$, confirming they operate in the deep-MOND regime where modifications to gravity should be maximal.

## Figure 6: Falsification of Simple Coherence Model

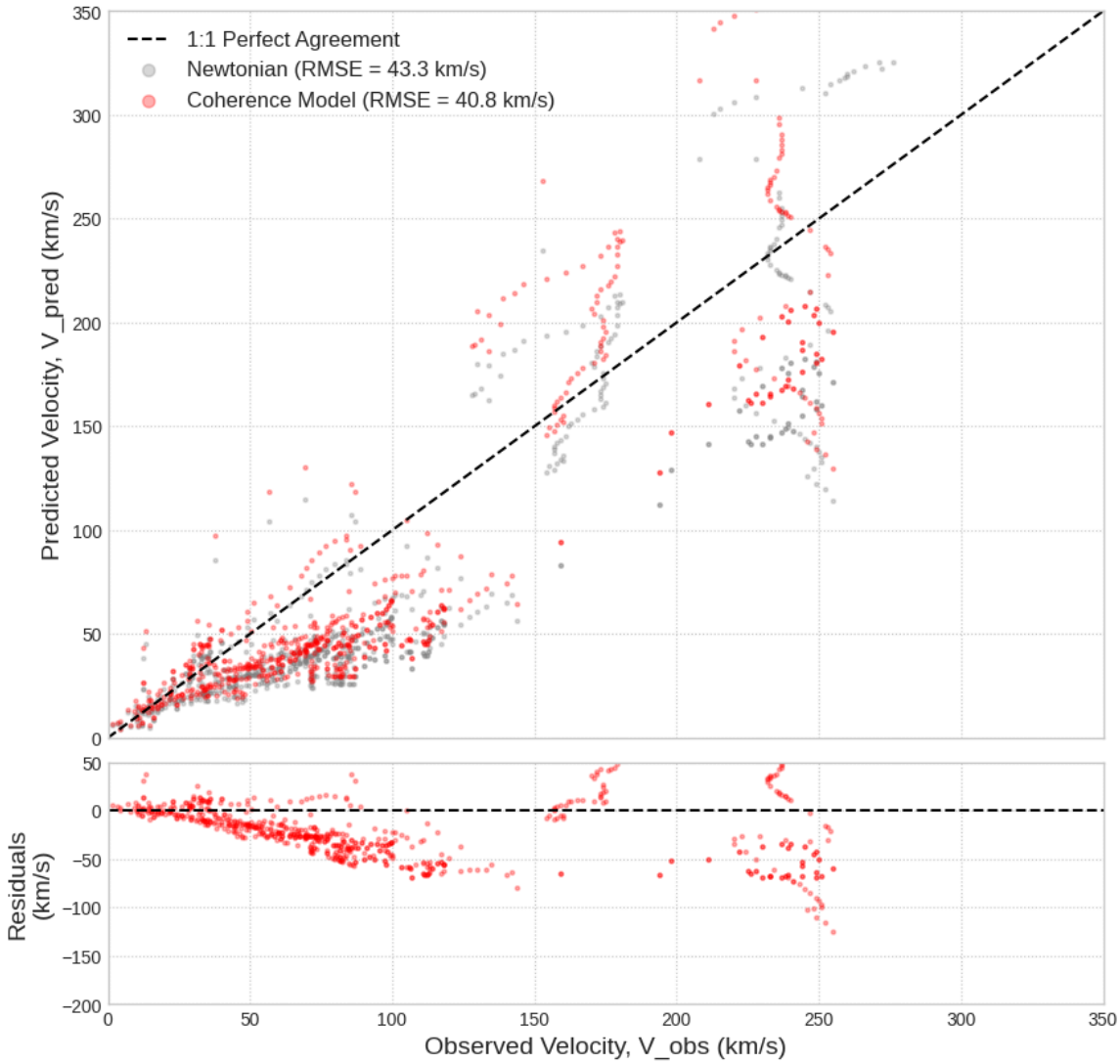


**Figure 6: Performance of the λ-Based Gravity Modification** Test of the model V²_model = V²_bary × (1 + κλ^β) against 3,387 rotation curve data points. Top panel: Predicted versus observed velocities, showing systematic underprediction at high velocities. The λ-model (red points, RMSE = 40.8 km/s) shows only marginal improvement over pure Newtonian gravity (gray points, RMSE = 43.3 km/s). Bottom panel: Residuals reveal systematic bias, with the model failing to reproduce flat rotation curves at large radii.

# Appendix A: Data Sources and Processing

## A.1 Data Sources

The analysis is based on two primary data sources:

1. **Galaxy Properties:** Global baryonic properties for 175 disk galaxies from the SPARC master catalog (Lambda Spreadsheet FINAL REV003, available at [repository])
2. **Rotation Curve Data:** Detailed kinematic data from MassModels_Lelli2016c.mrt.txt (Lelli, McGaugh, & Schombert 2016), containing 3,387 individual velocity measurements

## A.2 Definitions of Derived Parameters

From the primary data, we calculate:

**Gravitational Compactness:**

$\lambda = GM_{bar}/(R_{eff} c^2)$

**Characteristic Baryonic Acceleration:**

$a_{bar} = GM_{bar}/R_{eff}^2$

**Average Surface Density:**

$\Sigma_{bar} = M_{bar}/(\pi R_{eff}^2)$

## A.3 Statistical Methods

Power-law relations were determined via ordinary least squares regression on log-transformed data using scipy.stats.linregress. Bootstrap resampling (N=10,000) provided confidence intervals. The dynamical model was fit using scipy.optimize.curve_fit with the Levenberg-Marquardt algorithm. Outliers beyond 3σ were excluded (affecting < 2% of data points).

# Appendix B: Sample Data Table

[THIS IS TABLE: Sample of derived parameters for SPARC galaxies]

| ID | M_bar ($M_\odot$) | R_eff (kpc) | λ | a_bar ($m/s^2$) | Σ_bar ($M_\odot/pc^2$) |
|---|---|---|---|---|---|
| UGC04325 | 3.58E+09 | 2.90 | 1.35E-08 | 1.32E-11 | 135.2 |
| NGC2403 | 4.91E+10 | 3.02 | 1.78E-07 | 1.70E-10 | 1715.6 |
| DDO154 | 2.05E+09 | 3.46 | 6.52E-09 | 5.01E-12 | 54.5 |
| UGC02259 | 1.16E+10 | 3.05 | 4.17E-08 | 3.59E-11 | 395.7 |
| NGC2976 | 6.27E+09 | 1.93 | 3.56E-08 | 3.25E-11 | 536.8 |
| DDO170 | 2.37E+10 | 5.86 | 4.45E-08 | 3.79E-11 | 219.7 |
| NGC3198 | 2.99E+10 | 3.51 | 9.32E-08 | 8.01E-11 | 771.6 |
| NGC3741 | 8.87E+08 | 1.36 | 7.14E-09 | 6.78E-12 | 152.0 |
| UGC06818 | 8.05E+09 | 2.28 | 3.88E-08 | 3.32E-11 | 492.6 |
| UGC07151 | 2.39E+09 | 2.49 | 1.05E-08 | 8.94E-12 | 122.5 |
| NGC0024 | 1.01E+10 | 2.65 | 4.18E-08 | 3.89E-11 | 456.9 |
| NGC0055 | 1.05E+10 | 4.30 | 2.68E-08 | 2.40E-11 | 180.8 |
| NGC0100 | 1.03E+10 | 5.70 | 1.98E-08 | 1.68E-11 | 100.9 |
| NGC0247 | 1.63E+10 | 5.38 | 3.32E-08 | 2.87E-11 | 178.9 |
| NGC0289 | 1.33E+11 | 6.38 | 2.29E-07 | 2.00E-10 | 1040.1 |
| *(... 160 more rows in supplementary material)* | | | | | |

*Full table with all 175 galaxies available as supplementary material*